Biosensors and Bioelectronics 237 (2023) 115491

Contents lists available at ScienceDirect

Biosensors and Bioelectronics

journal homepage: www.elsevier.com/locate/bios

Optical glucose sensor for microfluidic cell culture systems☆

Stefanie Fuchs [a], Veronika Rieger [a], Anders Ø. Tjell [a], Sarah Spitz [b], Konstanze Brandauer [b], Roland Schaller-Ammann [c], Jürgen Feiel [c], Peter Ertl [b], Ingo Klimant [a], Torsten Mayr [a,*]

[a] Institute of Analytical Chemistry and Food Chemistry, Graz University of Technology, Stremayrgasse 9/II, 8010, Graz, Austria
[b] Institute of Applied Synthetic Chemistry and Institute of Chemical Technologies and Analytics, Faculty of Technical Chemistry, Vienna University of Technology, Getreidemarkt 9/163-164, 1060, Vienna, Austria
[c] HEALTH – Institute for Biomedical Research and Technologies, Joanneum Research Forschungsgesellschaft m.b.H, Neue Stiftingtalstraße 2, 8010, Graz, Austria

ARTICLE INFO

Keywords:
Microphysiological systems
Glucose
Optical sensor
Organ-on-Chip
Microfluidic
Flow through cell

ABSTRACT

Glucose is the primary energy source of human cells. Therefore, monitoring glucose inside microphysiological systems (MPS) provides valuable information on the viability and metabolic state of the cultured cells. However, continuous glucose monitoring inside MPS is challenging due to a lack of suitable miniaturized sensors. Here we present an enzymatic, optical glucose sensor element for measurement inside microfluidic systems. The miniaturized glucose sensor (Ø 1 mm) is fabricated together with a reference oxygen sensor onto biocompatible, pressure-sensitive adhesive tape for easy integration inside microfluidic systems. Furthermore, the proposed microfluidic system can be used as plug and play sensor system with existing MPS. It was characterized under cell culture conditions (37 °C and pH 7.4) for five days, exhibiting minor drift (3% day^{-1}). The influence of further cell culture parameters like oxygen concentration, pH, flow rate, and sterilization methods was investigated. The plug-and-play system was used for at-line measurements of glucose levels in (static) cell culture and achieved good agreement with a commercially available glucose sensor. In conclusion, we developed an optical glucose sensor element that can be easily integrated in microfluidic systems and is able to perform stable glucose measurements under cell culture conditions.

1. Introduction

In recent years, complex microfluidic cell culture systems attempt to mimic the (patho-) physiological environment of the human body. These so-called Organ-on-Chip or microphysiological systems (MPS) promise to model the human body better than animal models or static *in-vitro* cell cultures. Furthermore, integrated sensors allow to control these systems and will under-line our understanding of disease or drug mechanisms. Sensors for metabolic monitoring can provide insights into cell behavior in these systems (Fuchs et al., 2021; Kieninger et al., 2018). The key metabolic parameters oxygen and pH were successfully analyzed in microfluidic cell cultures (Fuchs et al., 2022; Zirath et al., 2021). Monitoring glucose in MPS would provide further valuable information on the viability and metabolic state of cultured cells (Kieninger et al., 2018; Ramadan and Zourob, 2020).

Many glucose sensing methods are based on the use of enzymes such as glucose oxidase (GOx). GOx catalyzes the reaction of glucose and oxygen to gluconolactone and hydrogen peroxide. This can be utilized as a sensor, either by measuring the produced hydrogen peroxide electrochemically, or the consumed oxygen with optical or electrochemical sensors. Both methods exhibit a cross sensitivity to oxygen and electrochemical sensors are prone to interference with other oxidizing species (Kieninger et al., 2018). Advanced electrochemical sensors use a mediator or transfer electrons directly from GOx to the electrode and optical sensors can use reference oxygen sensors to reduce oxygen dependency (Hassan et al., 2021; Pasic et al., 2006). The stability of the sensors is a further challenge, as it is dependent on the enzyme stability, which is affected by temperature and pH. Furthermore, the side product of the reaction, hydrogen peroxide, is known to deactivate enzymes and to influence cells in cell culture (Tric et al., 2017).

Particularly challenging for glucose monitoring in MPS are the integration, the size constrictions and the conditions in the sample. Miniaturized sensors are needed to fit into the microfluidic systems without generating too much dead volume. The sensors must provide

☆ Hereby we declare no conflicts of interest.

* Corresponding author.
E-mail address: torsten.mayr@tugraz.at (T. Mayr).

https://doi.org/10.1016/j.bios.2023.115491
Received 19 April 2023; Received in revised form 13 June 2023; Accepted 19 June 2023
Available online 25 June 2023

stable measurements at 37 °C for at least a few days, especially when integrated directly into the MPS. This poses problems with the lifetime of enzyme-based sensors. Furthermore, the sensors need to withstand sterilization and operate with the conditions set by the cell model, including flow speed, pH and glucose concentration. Typical glucose concentrations in cell culture media reach from 5 mM up to more than 30 mM glucose, and the glucose consumption inside the systems is usually low due to a decreased cell number or cell/media volume ratio. Thus, selecting the right measurement range while maintaining enough sensitivity to pick up changes in glucose consumption is challenging in MPS. Despite these challenges there were several approaches to measure glucose in MPS as it is a highly relevant parameter to control cell culture and monitor cells' metabolism.

First measurements of glucose in MPS were done with offline assays and enzymatic test stripe systems (Bauer et al., 2017; Lee et al., 2019; Moraes et al., 2013; Tanataweethum et al., 2022; Vahav et al., 2022). Both methods require sampling procedures and are not capable of in-line, continuous glucose monitoring. Additionally, commercially available electrochemical sensors were used for at-line and in-line measurements of glucose and lactate (Bavli et al., 2016; Matthiesen et al., 2022). These sensors required frequent recalibration and maintenance, making long-term measurements difficult. A first approach towards direct sensor integration in MPS was to fabricate custom electrochemical sensors on glass inserts that fit into a microfluidic hanging drop system (Misun et al., 2016). The sensors allowed in-line monitoring but were not suitable for measurements over 24 h. Dornhof et al. (2022) developed a microfluidic system for spheroid culture with integrated electrochemical sensors for oxygen, glucose, and lactate and reported measurements over six days of cell culture. Macroscopic optical glucose sensors have been successfully employed in static cell culture (Lederle et al., 2021; Tric et al., 2017). Overall, continuous glucose monitoring inside MPS is still challenging due to a lack of suitable, easy to integrate, miniaturized sensors.

We report an optical glucose sensor that is designed for measurements in microfluidic cell culture systems. The sensor can be integrated in microfluidic systems in two easy ways. It can be either integrated into the microfluidic cell culture device itself by sealing the system with the adhesive tape that supports the sensor, or in-line measurements can be conducted by connecting existing MPS to the microfluidic device that was used to characterized the sensor within this study. The enzymatic, diffusion limited, glucose sensor is based on the depletion of oxygen by glucose oxidase in the presence of glucose. Changes in oxygen concentration were measured via oxygen sensitive phosphorescent particles, which provided stable measurements in cell cultures before (Fuchs et al., 2022; Müller et al., 2021; Zirath et al., 2021). The addition of different catalysts was studied to remove the generated hydrogen peroxide and to improve sensor stability. An additional measure to increase enzymatic sensor stability is the use of diffusion limited sensors. These sensors feature an additional layer that limits the diffusion of glucose into the sensing layer, which is overloaded with GOx. Thus, enzyme activity and degradation do not affect this sensor type as there is an excess of enzyme used (Pasic et al., 2006; Tric et al., 2017). The sensitivity of these sensors is determined by the diffusion speed of glucose in the diffusion limiting layer. We integrated porous membranes as diffusion barriers for glucose to adapt the sensors measurement range. The miniaturized glucose sensing elements were fabricated together with an oxygen reference sensor to allow a compensation of changes in oxygen concentration during measurements. The influence of different catalysts, diffusion barriers, sterilization methods, and cell culture parameters such as flow rate, pH, and oxygen level on the sensor performance was investigated. Finally, the sensor was tested for long-term stability at 37 °C and measurements with static cell culture supernatant were performed and compared to a commercial sensor.

2. Material & methods

2.1. Buffer preparation

Chemicals were obtained from Carl Roth GmbH (Germany) if not stated otherwise. Phosphate buffered saline (PBS) was prepared in house containing 137 mM sodium chloride (NaCl)(AnalaR NORMAPUR, VWR Chemicals, USA), 2.7 mM potassium chloride (KCl), 10 mM di-sodium hydrogen phosphate dihydrate (Na2HPO4 · 2H2O), and 1.8 mM potassium dihydrogen phosphate (KH2PO4) (Merck KGaA, Germany). Its pH was adjusted to 7.4 at room temperature by using 1M NaOH or HCl.

100 mM or 1 M glucose stock solution was prepared by dissolving 1.982 mg D-(+)-Glucose monohydrate in 100 ml or 10 ml PBS. The solution was allowed to equilibrate over night before further usage. Glucose buffers were prepared by diluting the glucose stock solution in PBS.

2.1.1. Oxygen sensor preparation

Oxygen sensors were fabricated with slightly modified procedures as described previously (Fuchs et al., 2022; Zirath et al., 2021). Polystyrene beads were stained with an oxygen sensitive indicator dye platinum(II) meso-tetra(4-fluorophenyl) tetrabenzoporphyrin (Pt-TPTBPF) (Borisov et al., 2009; Nacht et al., 2015). 10% Hydromed D7 (AdvanSource Biomaterials, USA), a polyurethan based hydrogel, was dissolved in an ethanol water (9 + 1) mixture. The oxygen sensitive beads were homogenized within the dissolved hydrogel using a bead mill (Bead Ruptor 4, Omni International, USA) for 3 min at speed 3. The resulting sensor formulation had a 1:10 ratio of oxygen sensitive beads to dry mass of hydrogel. The liquid formulation was processed within 2 h.

2.2. Glucose sensor preparation

Glucose sensors were fabricated in a similar way to oxygen sensors. Additional to the hydrogel and oxygen sensitive particles, glucose oxidase cross-linked enzyme aggregates (GOx-CLEAs) were added to the sensor formulation. The GOx-CLEAs were obtained from B.Braun (Melsungen, Germany), and milled with the bead mill for 30s at maximum speed before addition of the remaining components. 10% Hydromed D7 solution, oxygen sensitive particles and ethanol were added. Furthermore, a catalyst for hydrogen peroxide degeneration was added. The enzyme catalase, as well as the two inorganic catalysts were tested in addition to the basic sensor composition without catalyst. The catalysts were prepared as follows before addition into the glucose sensor formulation.

i) Catalase (from bovine liver, Sigma-Aldrich, USA) was dissolved in PBS before addition.
ii) Pt-nanoparticles (Pt-NPs) were produced according to Ding et al. (2018) and added with PBS to the final mixture.
iii) Ruthenium (IV) oxide hydrate (Aldrich, USA) (RuO_2) was dispersed in 150 μL PBS using an ultrasonic water bath for 5 min. Fifty μL supernatant was removed before the remaining was added to the glucose sensor formulation.
iv) For sensors without additional catalyst PBS was added.

The final sensor formulations contained a dry weight ratio of GOx-CLEA + (No catalyst/Catalase/RuO_2/Pt-NPs) + oxygen sensitive particles + hydrogel of approximately 1 + (0/3/0.9/0.9) + 0.8 + 2. The mixtures were homogenized in the bead mill for 10s at maximum speed followed by 3 min at speed 3. The sensor formulations were used within 1 h after homogenization.

2.3. Sensor integration in microfluidic flow cell

The sensors were fabricated onto a biocompatible pressure sensitive adhesive tape (ThermalSeal RTS™, Excel Scientific, Inc., USA) using a

Table 1
PET Membrane properties.

Porosity	Pore density	Pore size	Thickness
0.3	$2*10^6$ cm^{-2}	0.4 μm	12 μm
0.5	$4*10^6$ cm^{-2}	0.4 μm	12 μm
1.6	$2*10^6$ cm^{-2}	1 μm	11 μm

microdispensing device (Gensheimer et al., in preparation). The microdispenser (MDS3200+, VERMES Microdispensing GmbH, Germany) was equipped with a nozzle with a diameter of 200 μm and a tungsten tapped (0.7 mm). The liquid sensor formulations were filled in the reservoir and forced to the nozzle using pressurized air with 400 mbar. The spotting parameters were adjusted to achieve sensor spots with a diameter between 600 μm and 800 μm. Typical spotting parameters for each sensor formulation can be found in Table SI 1. Oxygen and glucose sensors were fabricated with a center-to-center distance of 7.5 mm to fit the used microfluidic flow cell. After fabrication the sensors were allowed to dry over night before further use.

Porous polyethylene terephthalate (PET) membranes (ipCELLCULTURE™ Track Etched Membrane, it4ip S.A., Belgium) were used as diffusion barrier (specification see Table 1). The membranes were cut with 1.5 mm biopsy punching tools. After cutting, the membranes were placed centrally onto both sensors and fixated with slight pressure to the adhesive tape surrounding the sensing spot (Fig. 1 A). 3D printed microfluidic flow cells were obtained from Joanneum Research (Graz, Austria) (Schaller-Ammann et al., 2022). The adhesive tape with sensors is placed onto the flow cell to match the chambers of the microfluidic compartments with the sensors and fixed by applying slight pressure.

2.4. Sensor characterization

Sensor characterization was done under cell culture-like conditions (pH 7.4 and 37 °C) if not stated otherwise. The fluidic part of the setup was placed in a mini incubator (Labnet International, Inc., USA) to set the temperature to 37 °C during the measurement. Four flow cells containing the sensors were connected to a syringe pump (Cavro XLP Pump, Tecan, Switzerland) via a microfluidic manifold and PTFE tubing with an inner diameter of 0.3 mm. Each flow cell was connected such that the flow would first pass the oxygen sensor and then the glucose sensor, before it was finally guided through the outlet to the waste (Fig. 1 B). Optical fibers (Ø 1 mm) were fixated directly underneath the sensing spots onto the adhesive substrate (thickness: 50 μm polyolefin + 50 μm silicon adhesive) with custom-made holders for optical readout (Fig. 1 A, B). The phase fluorimeters (Firesting O2, Pyroscience GmbH, Germany), used for the readout, were stored outside the incubator as well as the pump unit. Temperature sensors (PT100, Pyroscience GmbH, Germany) were placed in the incubator to allow temperature compensation during the measurement. Flow cells with sensors were filled with PBS and stored at 37 °C over night to allow the sensor matrix to swell. The sensors were individually calibrated at air-saturated conditions with freshly injected PBS. The calibration under anoxic conditions was taken with 2% sodium sulfite in PBS on a spare sensor and the value was transferred to the other sensors. The glucose solutions, which were used for the characterization, were stored inside the incubator and connected to the pump. Each solution was flushed through the system before constant perfusion for more than 30 min during which the sensors response was assessed. The difference between the oxygen partial pressures measured by the reference oxygen sensor and the glucose sensor was used for further evaluation. Both the pumping process and the readout were performed completely automated so that no intervention in the setup was necessary.

2.4.1. Hydrogen depletion catalyst evaluation

Glucose solutions of 0, 1, 2, 3, 4 and 10 mM glucose and a flow of 0.25 μL/s were used for the characterization of sensors with and without a catalyst for the conversion of hydrogen peroxide. For stability evaluation this process was repeated at least once a day for three days. The stability of sensors without catalyst and with catalase was assessed with three calibrations per day, while the stability of sensors with RuO_2 and Pt-NPs was assessed with one calibration per day and a constant perfusion of 4 mM glucose buffer between calibrations.

2.4.2. Diffusion barrier

The glucose sensors were prepared with RuO_2 and sensors containing

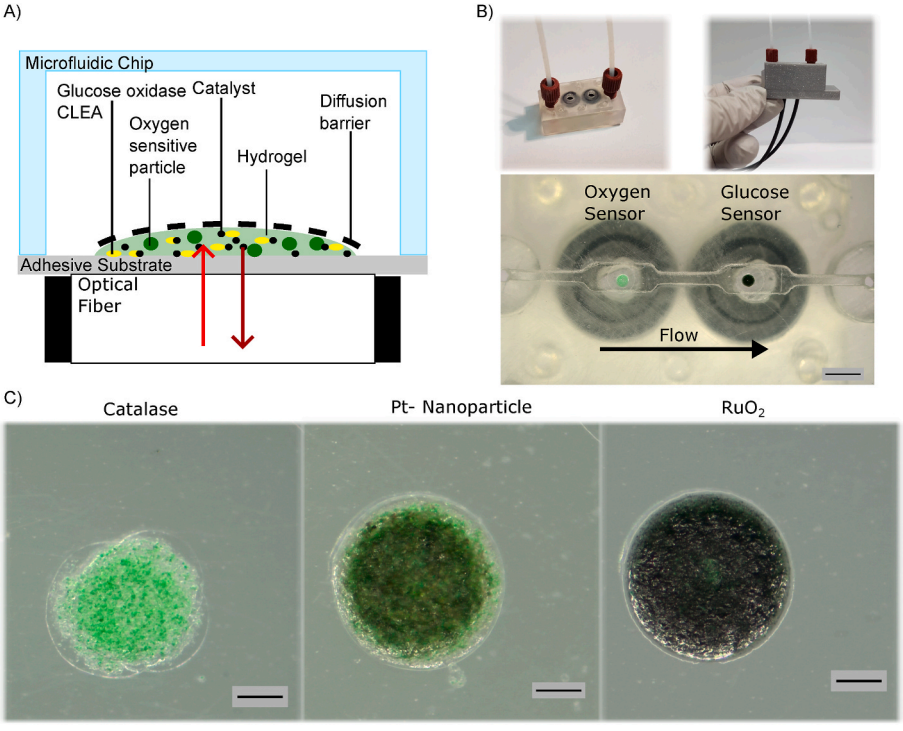

Fig. 1. A) The glucose sensors' sensing layer consists of GOx-CLEAs, particles stained with an oxygen sensitive dye and an additional catalyst for hydrogen peroxide degradation. All components were embedded in a hydrogel and covered by a porous membrane that acts as diffusion barrier. The sensor can be integrated in a microfluidic device using the adhesive sensor substrate. Optical fibers are fixed directly onto the sensor substrate for optical readout. B) Oxygen and glucose sensors were integrated into a microfluidic flow cell. The oxygen sensor was integrated into the first chamber and the glucose sensor in the second chamber in direction of the flow. Both sensors were equipped with a diffusion barrier with a diameter of 1.5 mm (scale bar 2 mm). Optical fibers were positioned on top of the sensors using a custom-made holder. C) Sensor spots with a diameter of 600–800 μm were produced from sensor formulations with different catalysts. Sensors containing Pt- NPs appear darker than sensors containing catalase and sensors containing RuO_2 appear black (scale bars 200 μm).

PET membranes with porosity of 1.6%, 0.5%, 0.3% (Table 1) were compared to sensors without membrane. For the evaluation glucose solutions with 0, 2.5, 5, 15, 20, 30 mM glucose and a flow velocity of 0.1 mm/s were used.

2.4.3. Influence of dissolved oxygen concentration

The influence of dissolved oxygen in the sample solution was investigated at room temperature. The sample was perfused with 10 μL/min through the flow cell via a microperfusion pump (MPP102, JOANNEUM RESEARCH Forschungsgesellschaft mbH, Austria) in a recirculating manner. The oxygen concentration of the sample was controlled by adjusting the inflow of nitrogen and pressurized air into the sample reservoir using two mass flow controllers (red-y smart series, Voegtlin, Switzerland). An oxygen microsensor (Pyroscience GmBH, Germany) was used to monitor the oxygen concentration in the sample. PEEK (polyetheretherketon) tubing guided the solution from the reservoir into the flow cell to reduce reoxygenation. The oxygen level of the sample solution was adjusted to either 100%, 75%, 25%, or 0% air saturation. After a sufficient equilibration time of the gas levels, the glucose levels were adjusted using a syringe pump to dispense defined amounts of glucose solution into the reservoir. A magnetic stirring bar was used to ensure sufficient mixing between PBS and the 1 M glucose solution. Glucose levels were adjusted to 2.5, 5, 7.5, 10 and 14 mM and kept for 35 min measurements. Afterward, the system was cleaned with PBS and reused.

2.4.4. pH influence

Glucose sensors with RuO_2 and diffusion barrier (1.6% porosity) were used for the evaluation of pH influence on the measurement. The sensors were allowed to swell in PBS (pH 7.4) overnight. PBS was adjusted to pH 6.5, 7.0, 7.4, 8.0 with 1M NaOH or HCl. The solutions were spiked with 1M glucose stock solution to achieve 0, 2.5, 5 and 10 mM Glucose in PBS. Calibration measurements were conducted at a flow rate of 0.08 μl/s for each pH in the following order pH 7.4, 7.0, 6.5, 7.4, 8.0.

2.4.5. Flow velocity

Flow cells were connected in series to the pump to ensure equal flow velocity in each cell. PBS with 5 mM glucose was perfused into the system at flow rates of 1.536, 0.768, 0.384, 0.192, 0.096, 0.048, 0.024, 0.012, 0.006, 0.003, 0 μL/s (equivalent to flow velocities of 2.05 mm/s to 0 mm/s). Each perfusion velocity was kept for 40 min. The measurement was repeated with buffers containing 10 mM, and 30 mM glucose.

2.4.6. Sterilization methods

Glucose sensors with RuO_2 and diffusion barrier underwent three different sterilization methods (UV, plasma, or electron beam irradiation) before they were integrated into flow cells. For UV treatment the sensors were placed in a laminar flow cabinet (Lorica, LAMSYSTEMS GmbH, Germany) with UV light turned on for 30 min. For oxygen plasma treatment, they were placed in a plasma oven (Diener electronic GmbH, Germany) which was evacuated for 3 min followed by oxygen flow for 3 min and plasma for 5 min. Electron beam irradiation was performed by treating the sensors with 25 kGy Beta irradiation by MediScan GmbH & Co KG (Austria). The treated sensors were compared to untreated sensors in measurements similar to those for characterization of the diffusion barrier.

2.4.7. Longterm characterization

Glucose sensors with RuO_2 and diffusion barrier (0.5% porosity) were used to evaluate the long-term stability of the sensors. The measurement was conducted simultaneously with 2 independent sensor systems (glucose sensor and oxygen reference). A calibration with glucose solutions of 0, 5, 10, 15 and 20 mM glucose with a flowrate of 0.16 μL/s was performed. Afterward, the sensors were perfused for 5 days with buffers containing 5, 10, 15, and 10 mM glucose in repetition. Each solution was perfused for 6 h at 0.16 μL/s.

2.4.8. Measurement of static cell culture supernatant

Cell culture medium was prepared by supplementing DMEM (11966025, Gibco, Germany) with 10% FBS (F9665, Sigma Aldrich, Austria), 1% antibiotics (penicillin and streptomycin, P4333, Sigma Aldrich, Austria), and 9 mM glucose (200 g/L D-glucose, Gibco, Germany). CaCo-2 cells were seeded in three cell densities in a 48-well tissue culture plate. 18 wells were seeded with 25000 c/cm^2, 50000 c/cm^2 and 100000 c/cm^2 respectively. All wells were covered with 400 μL medium. After 24 h the medium was exchanged in 27 out of the 54 wells. After 42 h the supernatant of all wells was collected for evaluation with the glucose sensors. Thus, media supernatants were evaluated after either 18 h or 42 h in cell culture. Three wells of each condition were pooled together, resulting in three pooled samples per condition.

The used glucose sensors contained RuO_2 and were covered with a diffusion barrier with 1.6% porosity. The sensors were integrated into flow cells and allowed to swell overnight in DMEM. The sample or calibration solution was guided into the flow cells using a peristaltic pump (205U, Watson-Marlow GmbH, UK) with a flow rate of 10 μL/min (Setup Figure SI 1). The calibration and the subsequent measurement were performed at room temperature. First oxygen calibration was performed with oxygenated DMEM without supplements. The anoxic condition was tested in an extra chip and the value was transferred to the other sensors. Afterward, the glucose calibration was performed by using 0, 3, 6, and 9 mM glucose in DMEM. After calibration, the cell culture samples were connected to the setup and measured. Three glucose sensors were used to measure one sample of each condition in parallel. Additionally, 2 μL of each sample were evaluated with a commercial glucose sensor (GlucCell, CESCO Bioengineering Co., LTD. Taiwan).

2.5. Data evaluation

All data evaluation was performed using python, including the pandas, numpy and scipy libraries. Evaluation of the different catalysts in the sensor formulation was performed without oxygen reference measurement. Therefore, the difference in oxygen partial pressure was assumed to be the difference between the measured value and the mean value of perfusion with PBS without glucose.

For all further evaluation oxygen sensors were integrated into the system and used as reference. The difference in oxygen partial pressure was determined as

$$\Delta pO_2 = pO_{2,Ref} - pO_{2,Glucose}$$

For calibration, the mean over minimum 15 min measurement of each glucose concentration was determined. Linear curve fits were performed using python scipy.optimize curve_fit and used for calibration. Values that are clearly associated with the presence of air bubbles in the system ($\Delta pO_2 < 5\ hPa$ and $c_{glucose} > 0\ mM$) were excluded from the evaluation. The limit of detection was determined as LOD = 3*std/slope. Measured values are given as mean ± standard deviation (std) of at least 3 samples if not stated otherwise.

3. Results and discussion

3.1. Sensing principle

The presented glucose sensors are enzymatic sensors and are based on the conversion of glucose to gluconolactone by GOx.

$$Glucose + O_2 \xrightarrow{GOx} Gluconolactone + H_2O_2$$

This reaction causes an oxygen depletion which is measured using the phosphorescent oxygen indicator dye. The glucose sensor consists of

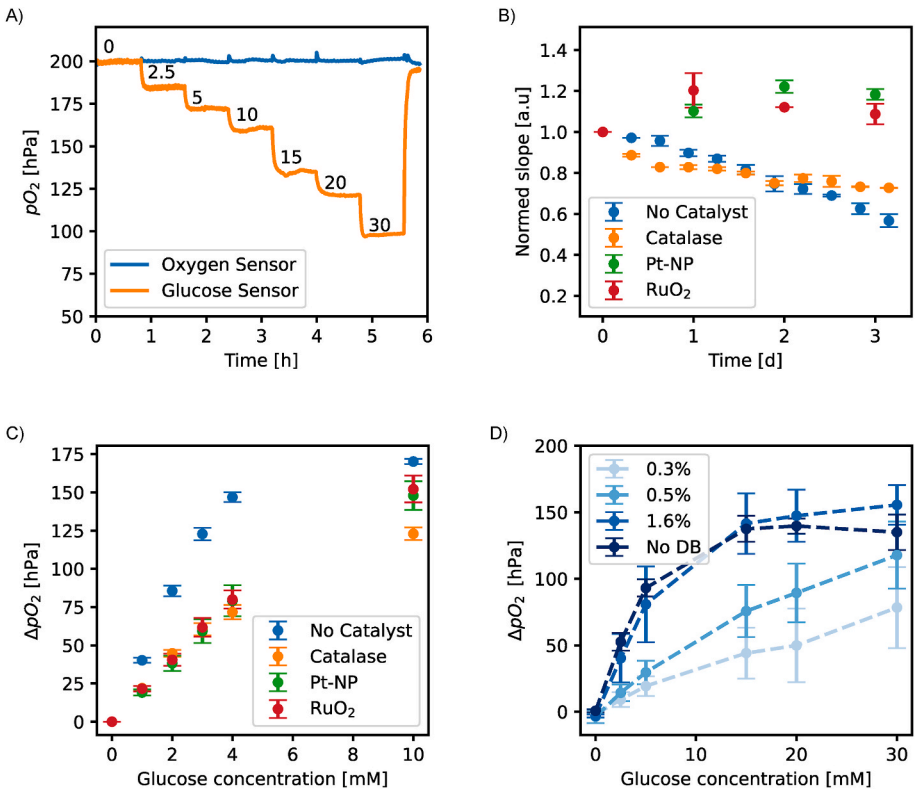

Fig. 2. Basic characterization of the glucose sensor. A) Response of a glucose sensor with a diffusion barrier (0.3% porosity) and oxygen reference sensor to different glucose concentrations from 0 to 30 mM. B) Influence of different hydrogen peroxide degenerating catalysts on the sensors stability over time, represented by the slope of the calibration function, and C) the sensors calibration. Sensors with catalase, platinum nanoparticles (Pt-NP) and ruthenium oxides (RuO_2) were compared to sensors without catalyst. D) Influence of the porosity of the PET membrane used as diffusion barrier on the calibration of the glucose sensors. Sensors with PET membranes with 0.3%, 0.5%, 1.6% porosity were compared to sensors without any diffusion barrier (No DB).

particles containing the oxygen sensitive phosphorescent dye and GOx-CLEAs which were immobilized in a biocompatible hydrogel (Fig. 1 A). Oxygen sensors without GOx were integrated prior to the glucose sensor in direction of the flow in the system to allow reference measurements of the samples oxygen content (Fig. 1 B). The difference (ΔpO_2) between the oxygen partial pressure measured by the reference sensor and the glucose sensor was used for further evaluation (Fig. 2 A). The by-product of the reaction, hydrogen peroxide, can affect the sensor lifetime by degenerating GOx. Therefore, one of the catalysts, catalase, Pt-NPs, or RuO2 was added into the sensor composition, to remove hydrogen peroxide. PET membranes were used to cover the sensor, limit the glucose diffusion and consequently change the measurement range and sensitivity of the sensor.

3.2. Sensor integration

Spotting parameters to fabricate glucose sensor spots with a diameter between 600 μm and 800 μm were established for all sensor compositions (Fig. 1 C). Even though glucose sensors containing RuO_2 appeared to be black, they gave sufficient phosphorescent signal strength to allow sensor readout when the optical fibers were well aligned with the sensor spot (Figure SI 2). The sensors were successfully integrated inside the microfluidic flow cell using the pressure sensitive adhesive tape (Fig. 1 B). This tape has been previously used in microfluidic systems for cell culture showing no adverse effects on the cells (Megarity et al., 2022; Serra et al., 2017). Furthermore, its feasibility to seal microfluidic chips made from various materials has been demonstrated (Serra et al., 2017). Consequently, the sensors can be easily integrated in media compartments of microfluidic chips if the media compartments face either the top or the bottom of the chip. Examples of the sensor integration into microfluidic devices using the adhesive substrate as well as connection examples of the flow cell with integrated sensors to other microfluidic chips using standard connectors and tubing can be found in the supplemental materials (Figure SI 3).

Glucose sensors, without catalyst for hydrogen peroxide degradation, showed a reversible behavior when exposed to glucose but a constant sensor degradation was observed. (Fig. 2 B, SI 4). This poor sensor stability is assumed to be caused by the degradation of the enzyme glucose oxidase by hydrogen peroxide. The introduction of catalysts for hydrogen peroxide degeneration into the glucose sensor changed its response to glucose (Fig. 2 C). All catalysts led to an apparent decrease in oxygen consumption of the glucose sensor. This behavior was expected, as the catalysts produce oxygen from hydrogen peroxide, thereby decreasing the overall oxygen consumption of the sensor. Before catalyst addition, sensors showed a steady decrease of the calibration slope over 3 days. Sensors with catalase also showed a decreasing slope over time, but it leveled off after two days. Contrary, sensors with inorganic catalysts showed an increase in the slope which stabilized after one day (Fig. 2 B). This increase might be due to a leaching of the catalyst from the sensor matrix. Overall, the sensor stability was increased by the addition of all tested hydrogen peroxide catalysts. The use of an inorganic catalyst is preferable over catalase to omit possible degradation of the enzyme catalase and thereby reducing the complexity of the sensor composition. For further characterization, the commercially available inorganic catalyst RuO_2 was chosen over the in-house synthesized Pt-NPs to simplify the production process.

The introduction of PET membranes with different porosities altered the sensor's response to glucose because the membranes were limiting the diffusion of glucose to the sensing material. A lower porosity of the membrane leads to less glucose diffusion. Sensors covered with the most porous membrane (1.6%) displayed a nearly similar response to sensors without membranes. The use of membranes with 0.3% and 0.5% porosity decreased the sensitivity but increased the measurement range of the sensor. Thus, the linear measurement range of the glucose sensor can be tuned to be 0 - < 10 mM using the membrane with 1.6% porosity or 0 - > 30 mM by using the other membranes (Fig. 2 D). The limits of detection were 0.7 ± 0.5 mM, 0.6 ± 0.6 mM and 0.2 ± 0.1 mM for membranes with 0.3%, 0.5%, 1.6% porosity, respectively. The addition of a diffusion barrier increased the sensor's footprint to 1.5 mm but a further miniaturization to 1 mm is possible (Figure SI 5) to allow sensor

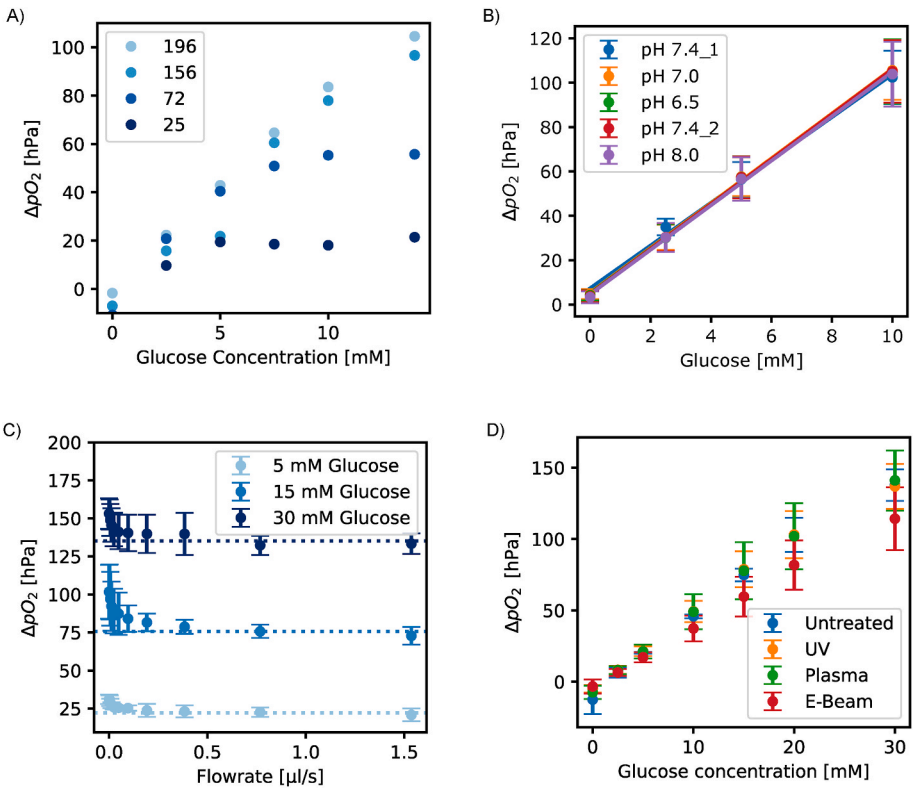

Fig. 3. Influence of cell culture parameters. A) Influence of dissolved oxygen in the sample on the glucose measurement. The legend depicts the available oxygen measured by the oxygen reference sensor in hPa. B) Influence of pH levels between 6.5 and 8.0 on the glucose sensor response. pH 7.4 is evaluated twice during the measurement indicated by '_1' or '_2' in the legend. The solid lines show the fitted curves that would be used for calibration. C) Flow rate dependency of glucose sensors; Response of glucose sensors to perfusion of PBS with 5 (light blue), 10 (blue), and 15 (dark blue) mM glucose at flow rates between 0 and 1.5 µL/s (flow velocity 0 mm/s −2 mm/s). D) Calibration curves of glucose sensors after different sterilization treatments. Untreated sensors are compared with sensors that underwent 30 min UV radiation, 5 min of oxygen plasma, or commercial electron beam radiation.

integration in smaller systems. Sensors with diffusion barriers showed a response time (t95) of 188 ± 53 s for changes of 5 mM glucose. This response time allows to monitor cell culture conditions as well as picking up changes in the metabolism of the cells over time (Bavli et al., 2016).

3.3. Influence of cell culture parameters on glucose measurements

The influence of basic microfluidic cell culture parameters and conditions such as dissolved oxygen, pH-value, flow rate, and sterilization, on the response of the glucose sensor with RuO_2 and diffusion barrier was investigated.

3.3.1. Oxygen concentration

Dissolved oxygen concentrations in microfluidic cell culture systems can vary due to several reasons, e.g. oxygen consumption of cultured cells or experimental induction of physiological or hypoxic conditions. The glucose sensors were calibrated under various oxygen concentrations to investigate the sensor behavior under these conditions (Fig. 3 A). Measurements below the glucose sensors' saturation level appeared to be unchanged, while a reduction of oxygen concentration inside the sample solution resulted in an earlier saturation of the glucose sensors and thus a decrease of the measurement range. The integrated oxygen reference sensor allows to compensate changes of the oxygen concentration inside the sample while measuring glucose. If large changes in oxygen concentration occur, which affect the limit of detection, it is possible to estimate the new upper limit of detection using the oxygen reference sensor. Furthermore, the oxygen reference sensor can be used to assess the oxygen consumption of the cultivated cells if the sensors are integrated in close proximity to the cells in an MPS. In case of the proposed plug-and-play system a measurement of oxygen consumption of the cultivated cells is not possible due to sample reoxygenation inside the system before reaching the oxygen sensor.

3.3.2. pH-value

The pH level of the sample solution did not influence the glucose sensors' response between the tested pH levels (pH 6.5 to 8.0) (Fig. 3 B). Cell culture medium usually contains strong buffer systems to prevent huge pH changes, thus allowing for glucose measurements in the tested pH range. However, the integration of pH sensors in the system might be helpful to detect pH drops below the tested range, which might affect the sensor as well as the cells. Furthermore, pH is also a viable indicator of the metabolic state of cells, therefore allowing further insights into cellular metabolism. Optical pH sensors that have been previously published by our group (Fuchs et al., 2022; Müller et al., 2021) are spectrally compatible with the developed glucose sensor and fabricated in the same manner thereby making integration and readout easily possible without further equipment. pH measurements will allow pH monitoring and control in less buffered systems.

3.3.3. Flow rates

The system was tested at flow rates that are typically used in microfluidic systems for cell culture (1.536 µL/s - 0.003 µL/s). Low flow rates increased the sensor's sensitivity because less oxygen is transported to the sensor side via the fluid flow (Fig. 3 C). Thus, calibrating the sensor at the same flow rate that will be used in the cell culture system and further a constant flow throughout the measurement will be necessary. When higher flow rates (>0.4 µL/s) are used, the sensor shows only little or no flow dependency. Overall, this shows the suitability of the system to measure glucose as plug and play sensor chip inside the perfusion system of an MPS. Furthermore, the tested flow rates correspond to flow velocities which are also typically used inside MPS, suggesting the integration of the sensors directly in the media channel of an MPS.

3.3.4. Sterilization

Sterilization or disinfection is necessary if the sensors are used in cell culture. The usage of 70% Ethanol solution for disinfection is not possible as the sensors will degrade. Other commonly used treatments like UV, plasma, or electron beam radiation are compatible with the sensors. UV treatment and treatment with oxygen plasma for

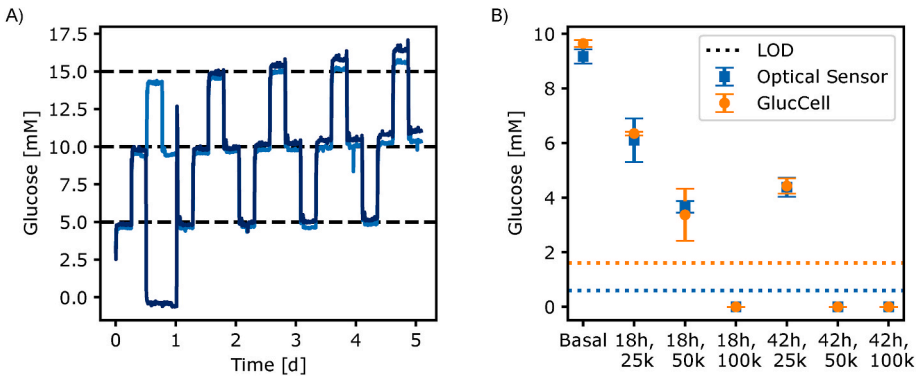

Fig. 4. A) Evaluation of sensor stability by alternating perfusion of 5 mM, 10 mM, and 15 mM glucose in PBS over a period of 5 days. One of the sensors (dark blue) is covered by an air bubble from 0.5 d to 1 d resulting in an apparent measurement of 0 mM glucose. B) Measurement of static cell culture supernatant at basal conditions, and after culture of 25000, 50000, and 100000 cells for 18 or 42 h. Results from the developed optical sensors (blue) are compared to results from a commercially available glucose sensor (GlucCell, orange). The dotted lines denote the limits of detection of the sensors (developed sensor 0.6 mM, commercial sensor 1.6 mM). Results below the limit of detection are visualized as 0.

Table 2
Comparison of selected glucose sensors for cell-culture application.

Reference	Sensing method	Dynamic range	Sensitivity	Limit of Detection	Response time	Stability	Size
This publication	Optical	0 - >30 mM 0 - >30 mM 0 –10 mM	3.0 ± 0.7 hPa mM^{-1} 4.0 ± 0.7 hPa mM^{-1} 11.1 ± 2.7 hPa mM^{-1}	0.7 ± 0.5 mM, 0.6 ± 0.6 mM 0.2 ± 0.1 mM	T95 188 ± 53 s	5 days at 37 °C (drift 3%/day)	Ø 1.0 mm
Dornhof et al. (2022)	Amperometric	physiological range	3.8 nA mM^{-1} mm^{-2}	7.6 ± 3.7 µM	n.s.	Cell-culture over 6 days shown	Ø 300 µm (working electrode)
Misun et al. (2016)	Amperometric	0–2 mM 0–7 mM 0–11 mM	322 ± 41 nA mM^{-1} mm^{-2} 88 nA mM^{-1} mm^{-2} 30 nA mM^{-1} mm^{-2}	n.s.	n.s.	1 day	Ø 400 µm (working electrode)
Tang et al. (2020)	Amperometric	0–2 mM	5.7 ± 0.3 µA cm^{-2} mM^{-1}	0.004 mM	n.s.	30 consecutive measurements	Ø 3 mm (Working electrode)
Tric et al. (2017)	Optical	0–20 mM	n.s.	0.45 mM	T90 < 10min	>52 d at RT	n.s.

n.s. = not stated; RT = room temperature.

disinfection did not affect the sensor performance illustrated by calibration curves obtained after the sterilization method in Fig. 3 D. Whereas, the commercially preferred electron beam radiation slightly affected the sensor. However, the sensors still showed a suitable response to glucose. To summarize, all tested sterilization methods were suitable for the treatment of the glucose sensors but calibration after sterilization will be necessary.

3.3.5. Long term stability and measurement of cell culture supernatant

Glucose sensors displayed a stable performance over the course of 5 days with a drift of 2.1% ± 0.7% per day (N = 2) (Fig. 4 A) at a constant temperature of 37 °C. This linear drift behavior will allow drift compensation in future measurements. Measurements of cell culture supernatant were in good agreement with a commercial sensor. The measurement of cell culture medium at basal conditions without cells with the developed optical sensors measured 9.2 ± 0.3 mM glucose while the commercial sensor measured 9.6 ± 0.1 mM glucose. Samples with increased cell density and culture time showed decreasing glucose levels with both methods, as expected. Furthermore, three sample conditions were below the LOD for both devices (0.6 mM developed sensors, 1.6 mM commercial sensor, Fig. 4 B). Overall, the data showed the ability of the glucose sensors to measure cell culture medium in relevant glucose concentrations. A comparison of the developed glucose sensors to other glucose sensors, which are proposed for measurments within cell-culture, can be found in Table 2.

4. Conclusion

We report on an optical glucose sensor that is designed for measurements in microfluidic cell culture systems. The miniaturized glucose sensors (Ø 1 mm) and oxygen reference sensors can be easily integrated into microfluidic systems by sealing the system with the adhesive sensor substrate. Furthermore, the shown microfluidic setup can be used as a plug-and-play sensor chip with existing systems. The sensor system showed stable measurements over a course of 5 days with a drift of less than 3% per day at 37 °C. The glucose sensors withstand commonly used sterilization methods and can be operated in cell culture medium with reduced oxygen levels, over a wide range of flow rates. Both the available oxygen level and the flow velocity affect the sensitivity and the measurement range of the glucose sensor. Therefore, the adaptation of the sensor to different measurement ranges via the diffusion barrier must be chosen carefully with respect to the used cell culture medium, flow velocity, and possible oxygen depletion from the medium. No influence of the pH was seen on the measurement between pH 6.5 and 8.0, but further investigation needs to be done outside of this range. However, glucose measurements are possible using well-buffered systems. Experiments with static cell culture supernatant showed that the developed sensors were in good agreement with a commercially available glucose sensor. The sensors will be integrated into more complex MPS in future experiments to allow cell culture control and monitoring of cellular glucose consumption. Furthermore, the system can be expanded with optical pH sensors and oxygen sensors which are integrated in close proximity to the cells to enable measurement of the extracellular acidification rate and the oxygen consumption of the cells. This will allow multiparametric monitoring of metabolic relevant parameters, using one device.

CRediT authorship contribution statement

Stefanie Fuchs: Conceptualization, Methodology, Investigation, Formal analysis, Visualization, Writing – original draft, Writing – review & editing. **Veronika Rieger:** Investigation. **Anders Ø. Tjell:** Methodology, Nanoparticle Synthesis. **Sarah Spitz:** Methodology, Cell culture, Investigation. **Konstanze Brandauer:** Methodology, Cell culture,

Investigation. **Roland Schaller-Ammann:** Methodology, Flow cell. **Jürgen Feiel:** CAD-renderings. **Peter Ertl:** Writing – review & editing, Resources. **Ingo Klimant:** Conceptualization. **Torsten Mayr:** Conceptualization, Supervision, Funding acquisition, Writing – review & editing.

Declaration of competing interest

The authors declare the following financial interests/personal relationships which may be considered as potential competing interests: Torsten Mayr reports a relationship with PyroScience GmbH that includes: board membership, employment, and equity or stocks. Ingo Klimant reports a relationship with PyroScience GmbH that includes: board membership and equity or stocks.

Data availability

Data will be made available on request.

Acknowledgement

This work has received funding from the European Union's Horizon 2020 research and innovation programme under the Marie Skłodowska-Curie grant agreement No 812954.

Appendix A. Supplementary data

Supplementary data to this article can be found online at https://doi.org/10.1016/j.bios.2023.115491.

References

Bauer, S., Wennberg Huldt, C., Kanebratt, K.P., Durieux, I., Gunne, D., Andersson, S., Ewart, L., Haynes, W.G., Maschmeyer, I., Winter, A., Ämmälä, C., Marx, U., Andersson, T.B., 2017. Functional coupling of human pancreatic islets and liver spheroids on-a-chip: towards a novel human ex vivo type 2 diabetes model. Sci. Rep. 7, 14620 https://doi.org/10.1038/s41598-017-14815-w.

Bavli, D., Prill, S., Ezra, E., Levy, G., Cohen, M., Vinken, M., Vanfleteren, J., Jaeger, M., Nahmias, Y., 2016. Real-time monitoring of metabolic function in liver-on-chip microdevices tracks the dynamics of mitochondrial dysfunction. Proc. Natl. Acad. Sci. U. S. A. 113, E2231–E2240. https://doi.org/10.1073/pnas.1522556113.

Borisov, S.M., Nuss, G., Haas, W., Saf, R., Schmuck, M., Klimant, I., 2009. New NIR-emitting complexes of platinum(II) and palladium(II) with fluorinated benzoporphyrins. J. Photochem. Photobiol. Chem. 201, 128–135. https://doi.org/10.1016/j.jphotochem.2008.10.003.

Ding, L., Chen, S., Zhang, W., Zhang, Y., Wang, X., 2018. Fully reversible optical sensor for hydrogen peroxide with fast response. Anal. Chem. 90, 7544–7551. https://doi.org/10.1021/acs.analchem.8b01159.

Dornhof, J., Kieninger, J., Muralidharan, H., Maurer, J., Urban, G.A., Weltin, A., 2022. Microfluidic organ-on-chip system for multi-analyte monitoring of metabolites in 3D cell cultures. Lab Chip 22, 225–239. https://doi.org/10.1039/D1LC00689D.

Fuchs, S., Johansson, S., Tjell, A.Ø., Werr, G., Mayr, T., Tenje, M., 2021. In-line analysis of organ-on-chip systems with sensors: integration, fabrication, challenges, and potential. ACS Biomater. Sci. Eng. 7, 2926–2948. https://doi.org/10.1021/acsbiomaterials.0c01110.

Fuchs, S., van Helden, R.W.J., Wiendels, M., de Graaf, M.N.S., Orlova, V.V., Mummery, C.L., van Meer, B.J., Mayr, T., 2022. On-chip analysis of glycolysis and mitochondrial respiration in human induced pluripotent stem cells. Mater. Today Bio 17, 100475. https://doi.org/10.1016/j.mtbio.2022.100475.

Gensheimer, T., Fuchs, S., Vermeul, K., Mayr, T., Passier, R., Van Der Meer, A.D., in Preparation. Microfluidic Chips with Local Oxygen Sensors Demonstrate Time-dependent Changes in Oxygen Concentrations during the Formation of Functional 3D Vascular Networks.

Hassan, M.H., Vyas, C., Grieve, B., Bartolo, P., 2021. Recent advances in enzymatic and non-enzymatic electrochemical glucose sensing. Sensors 21, 4672. https://doi.org/10.3390/s21144672.

Kieninger, J., Weltin, A., Flamm, H., Urban, G.A., 2018. Microsensor systems for cell metabolism – from 2D culture to organ-on-chip. Lab Chip 18, 1274–1291. https://doi.org/10.1039/C7LC00942A.

Lederle, M., Tric, M., Roth, T., Schütte, L., Rattenholl, A., Lütkemeyer, D., Wölfl, S., Werner, T., Wiedemann, P., 2021. Continuous optical in-line glucose monitoring and control in CHO cultures contributes to enhanced metabolic efficiency while maintaining darbepoetin alfa product quality. Biotechnol. J. 16, 2100088 https://doi.org/10.1002/biot.202100088.

Lee, D.W., Lee, S.H., Choi, N., Sung, J.H., 2019. Construction of pancreas–muscle–liver microphysiological system (MPS) for reproducing glucose metabolism. Biotechnol. Bioeng. 116, 3433–3445. https://doi.org/10.1002/bit.27151.

Matthiesen, I., Nasiri, R., Tamashiro Orrego, A., Winkler, T.E., Herland, A., 2022. Metabolic assessment of human induced pluripotent stem cells-derived astrocytes and fetal primary astrocytes: lactate and glucose turnover. Biosensors 12, 839. https://doi.org/10.3390/bios12100839.

Megarity, D., Vroman, R., Kriek, M., Downey, P., Bushell, T.J., Zagnoni, M., 2022. A modular microfluidic platform to enable complex and customisable in vitro models for neuroscience. Lab Chip 22, 1989–2000. https://doi.org/10.1039/D2LC00115B.

Misun, P.M., Rothe, J., Schmid, Y.R.F., Hierlemann, A., Frey, O., 2016. Multi-analyte biosensor interface for real-time monitoring of 3D microtissue spheroids in hanging-drop networks. Microsyst. Nanoeng. 2, 1–9. https://doi.org/10.1038/micronano.2016.22.

Moraes, C., Labuz, J.M., Leung, B.M., Inoue, M., Chun, T.-H., Takayama, S., 2013. On being the right size: scaling effects in designing a human-on-a-chip. Integr. Biol. 5, 1149. https://doi.org/10.1039/c3ib40040a.

Müller, B., Sulzer, P., Walch, M., Zirath, H., Buryška, T., Rothbauer, M., Ertl, P., Mayr, T., 2021. Measurement of respiration and acidification rates of mammalian cells in thermoplastic microfluidic devices. Sensor. Actuator. B Chem. 334, 129664 https://doi.org/10.1016/j.snb.2021.129664.

Nacht, B., Larndorfer, C., Sax, S., Borisov, S.M., Hajnsek, M., Sinner, F., List-Kratochvil, E.J.W., Klimant, I., 2015. Integrated catheter system for continuous glucose measurement and simultaneous insulin infusion. Biosens. Bioelectron. 64, 102–110. https://doi.org/10.1016/j.bios.2014.08.012.

Pasic, A., Koehler, H., Schaupp, L., Pieber, T.R., Klimant, I., 2006. Fiber-optic flow-through sensor for online monitoring of glucose. Anal. Bioanal. Chem. 386, 1293–1302. https://doi.org/10.1007/s00216-006-0782-x.

Ramadan, Q., Zourob, M., 2020. Organ-on-a-chip engineering: toward bridging the gap between lab and industry. Biomicrofluidics 14, 041501. https://doi.org/10.1063/5.0011583.

Schaller-Ammann, R., Kreß, S., Feiel, J., Schwagerle, G., Priedl, J., Birngruber, T., Kasper, C., Egger, D., 2022. Advanced online monitoring of in vitro human 3D full-thickness skin equivalents. Pharmaceutics 14, 1436. https://doi.org/10.3390/pharmaceutics14071436.

Serra, M., Pereiro, I., Yamada, A., Viovy, J.-L., Descroix, S., Ferraro, D., 2017. A simple and low-cost chip bonding solution for high pressure, high temperature and biological applications. Lab Chip 17, 629–634. https://doi.org/10.1039/C6LC01319H.

Tanataweethum, N., Trang, A., Lee, C., Mehta, J., Patel, N., Cohen, R.N., Bhushan, A., 2022. Investigation of insulin resistance through a multiorgan microfluidic organ-on-chip. Biomed. Mater. 17, 025002 https://doi.org/10.1088/1748-605X/ac4611.

Tang, Y., Petropoulos, K., Kurth, F., Gao, H., Migliorelli, D., Guenat, O., Generelli, S., 2020. Screen-printed glucose sensors modified with cellulose nanocrystals (CNCs) for cell culture monitoring. Biosensors 10, 125. https://doi.org/10.3390/bios10090125.

Tric, M., Lederle, M., Neuner, L., Dolgowjasow, I., Wiedemann, P., Wölfl, S., Werner, T., 2017. Optical biosensor optimized for continuous in-line glucose monitoring in animal cell culture. Anal. Bioanal. Chem. 409, 5711–5721. https://doi.org/10.1007/s00216-017-0511-7.

Vahav, I., Thon, M., van den Broek, L.J., Spiekstra, S.W., Atac, B., Lindner, G., Schimek, K., Marx, U., Gibbs, S., 2022. Proof-of-Concept organ-on-chip study: topical cinnamaldehyde exposure of reconstructed human skin with integrated neopapillae cultured under dynamic flow. Pharmaceutics 14, 1529. https://doi.org/10.3390/pharmaceutics14081529.

Zirath, H., Spitz, S., Roth, D., Schellhorn, T., Rothbauer, M., Müller, B., Walch, M., Kaur, J., Wörle, A., Kohl, Y., Mayr, T., Ertl, P., 2021. Bridging the academic–industrial gap: application of an oxygen and pH sensor-integrated lab-on-a-chip in nanotoxicology. Lab Chip 10. https://doi.org/10.1039/D1LC00528F, 1039.D1LC00528F.